

**Ab initio study of ferroelectricity in edged PbTiO<sub>3</sub> nanowires under axial tension**

Takahiro Shimada,\* Shogo Tomoda, and Takayuki Kitamura  
 Graduate School of Engineering, Kyoto University, Sakyo-ku, Kyoto 606-8501, Japan  
 (Received 16 June 2008; published 6 January 2009)

The atomistic and electronic structures of PbTiO<sub>3</sub> nanowires with characteristic edges consisting of (100) and (010) surfaces and the crucial role of axial tensile strain on ferroelectricity have been investigated by means of *ab initio* density-functional theory calculations. Ferroelectricity is enhanced at the edge of the PbO-terminated nanowire because the Pb-O covalent bond that predominates ferroelectric distortions is locally strengthened. On the other hand, a considerable suppression is found in the TiO<sub>2</sub>-terminated nanowire, caused by the charge transfer from the Pb-O site to the Ti-O site. Surprisingly, the smallest PbO-terminated nanowire with a cross section of only one-unit cell can possess ferroelectricity while ferroelectricity disappears in the TiO<sub>2</sub>-terminated nanowires with a cross section smaller than four-by-four cells (diameter of about 17 Å). However, ferroelectricity is recovered by axial tension, where smaller nanowires require larger critical strains.

DOI: 10.1103/PhysRevB.79.024102

PACS number(s): 77.80.-e, 61.46.Km, 31.15.A-

**I. INTRODUCTION**

Ferroelectric (FE) nanowires have drawn much attention as one-dimensional multifunctional materials for technological applications, e.g., ferroelectric random access memories (FeRAMs).<sup>1,2</sup> In recent years, single-crystalline PbTiO<sub>3</sub> and BaTiO<sub>3</sub> nanowires with a diameter of 5–12 nm have been manufactured,<sup>3–5</sup> and smaller nanowires with several lattice spacings are anticipated in the near future. Nanowires fabricated on a substrate have an atomically sharp edge structure consisting of (100) and (010) perovskite surfaces.<sup>6</sup> Moreover, the edge structure is commonly observed in nanostructured perovskite-type oxides, e.g., the step on the SrTiO<sub>3</sub> (001) surface,<sup>7,8</sup> the “zigzag” (110) surface structure,<sup>9</sup> and the edge of a PbTiO<sub>3</sub> nanoisland.<sup>10,11</sup> Thus, the edges are among the characteristic nanostructures in perovskite oxides.

Ferroelectricity, which originates from the complex balance between short-range covalent and long-range Coulomb interactions,<sup>12,13</sup> is very sensitive to the shape and size of nanostructured materials as well as the mechanical deformation.<sup>14</sup> Since the coordination number rapidly decreases at the edge in nanowires, the balance of both interactions differs considerably from that in the bulk. Hence, the edge structure can strongly affect ferroelectricity, especially in a thin nanowire where the ratio of the edge with respect to the entire volume is quite high. In addition, nanowires are normally subjected to axial tension or compression, which sometimes recovers or destabilizes the ferroelectric distortions.<sup>15,16</sup> Thus, ferroelectricity in the edged nanowire and its response to the axial strain are fundamental issues and worth investigating.

Geneste *et al.*<sup>17</sup> studied the finite-size effects in BaTiO<sub>3</sub> nanowires with an edge structure using *ab initio* (first-principles) calculations based on the density-functional theory (DFT),<sup>18,19</sup> and revealed a critical diameter for ferroelectricity. However, the situation may differ in the case of PbTiO<sub>3</sub> where the ferroelectric instability is quite different from that in BaTiO<sub>3</sub>.<sup>20</sup> Moreover, the termination layer of the PbTiO<sub>3</sub> (001) surface has immense influence on ferroelectricity<sup>21–23</sup> while a moderate effect is found in the case of BaTiO<sub>3</sub> surface.<sup>21,24</sup> Thus, it is also necessary to in-

vestigate how ferroelectricity in the PbTiO<sub>3</sub> nanowire is affected by terminations making up the edge structure.

In this paper, we study PbTiO<sub>3</sub> nanowires with atomically sharp edges consisting of (100) and (010) surfaces by means of *ab initio* density-functional theory calculations in order to elucidate the intrinsic effects of edges on ferroelectricity. In addition, the finite-size dependence and the crucial role of the axial tensile strain are investigated. This paper is organized as follows. In Sec. II, we describe the details of the simulation procedure. In Sec. III, the relaxed atomic configuration and electronic structure of the PbTiO<sub>3</sub> nanowires are presented, and the site-by-site ferroelectric distortions are discussed by focusing on the edge. We also investigate the effect of wire size on ferroelectricity. Furthermore, we discuss the ferroelectric behavior under axial tension and present the critical strain. Finally, the results are summarized in Sec. IV.

**II. COMPUTATIONAL DETAILS****A. Simulation method**

*Ab initio* calculations based on the density-functional theory<sup>18,19</sup> are conducted using the Vienna *Ab initio* Simulation Package (VASP).<sup>25,26</sup> The electronic wave functions are expanded in-plane waves up to a cutoff energy of 500 eV. The pseudopotentials based on the projector augmented wave (PAW) method<sup>27</sup> explicitly include the O 2*s* and 2*p*, the Ti 3*s*, 3*p*, 3*d*, and 4*s*, and the Pb 5*d*, 6*s*, and 6*p* electrons in the valence states. The local-density approximation (LDA) of the Ceperley-Alder form<sup>28</sup> is employed to evaluate the exchange-correlation energy.

**B. Simulation models and procedure**

We study PbTiO<sub>3</sub> nanowires with edges consisting of (100) and (010) surfaces, where there are two possible terminations of the PbO and TiO<sub>2</sub> atomic layers. Figures 1(a) and 1(b) show the simulation models of the PbO-terminated and TiO<sub>2</sub>-terminated nanowires, respectively. Each nanowire has a cross section in which four perovskite unit cells are arranged in the *x* and *y* directions, which is denoted as the

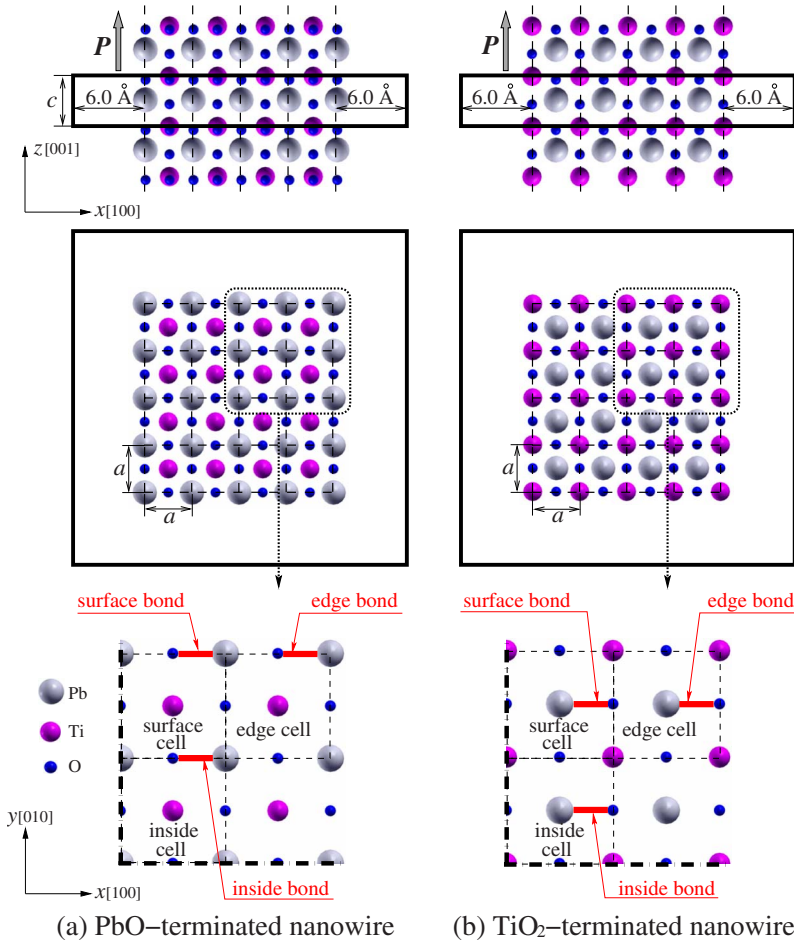


FIG. 1. (Color online) Simulation models of (a) PbO-terminated and (b) TiO<sub>2</sub>-terminated nanowires with a cross section of  $4 \times 4$  unit cells. The solid boxes represent the simulation cells. Spontaneous polarization  $\mathbf{P}$  lies along the  $z$  (axial) direction. The Pb-O bonds in the edge, surface, and inside cells are referred to edge, surface, and inside bonds, respectively.

cross section of  $4 \times 4$  unit cells below. Spontaneous polarization aligns along the  $z$  direction (the axial direction in the nanowire). Since a three-dimensional periodic boundary condition is applied in the calculations, a vacuum region of  $l_v = 12 \text{ \AA}$  thickness is introduced in both the  $x$  and  $y$  directions so that undesirable interaction between the neighboring nanowires is sufficiently avoided. The simulation cell dimensions in the  $x$ ,  $y$ , and  $z$  directions are initially set to  $4a + l_v$ ,  $4a + l_v$ , and  $c$ , respectively, where the theoretical lattice constants of the tetragonal bulk,  $a = 3.867 \text{ \AA}$  and  $c = 4.034 \text{ \AA}$  ( $c/a = 1.043$ ), are used. The Brillouin-zone (BZ) integration is carried out with a  $2 \times 2 \times 6$   $k$ -point mesh generated by the Monkhorst-Pack scheme.<sup>29</sup>

The unit cells at an edge, on a surface, and inside the nanowire are referred to as “edge cell,” “surface cell,” and “inside cell,” respectively (see Fig. 1). The terms “edge bond,” “surface bond,” and “inside bond” denote the Pb-O covalent bonds in the corresponding cells for descriptive purpose.

To obtain an equilibrium structure, atomic positions and a cell size in the  $z$  direction are fully relaxed using the conjugate gradient method until all the Hellmann-Feynman forces and the stress component  $\sigma_{zz}$  are less than  $1.0 \times 10^{-3} \text{ eV/\AA}$  and  $1.0 \times 10^{-2} \text{ GPa}$ , respectively.

Smaller nanowires with cross sections of  $1 \times 1$ ,  $2 \times 2$ , and  $3 \times 3$  unit cells are investigated in the same manner in order to elucidate the effects of nanowire size and axial strain on ferroelectricity. For tensile simulations, a small axial strain,

$\Delta \varepsilon_{zz}$ , is applied to the simulation cell step by step. At each strain, internal atoms are fully relaxed under the fixed cell dimensions.

### III. RESULTS AND DISCUSSION

#### A. Ferroelectricity in unstrained nanowires

We introduce a local polarization in two fictitious Pb-edged and Ti-edged “unit cells” as illustrated in Fig. 2 for PbO-terminated and TiO<sub>2</sub>-terminated nanowires, respectively. The local polarization in the cell,  $\mathbf{P}$ , is evaluated by

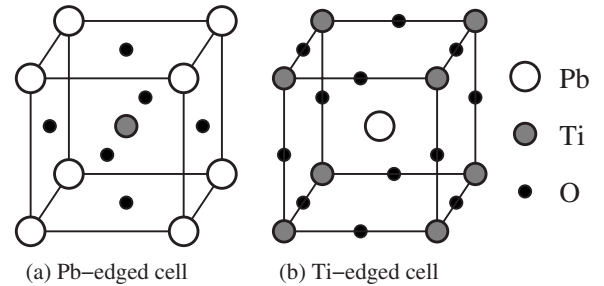


FIG. 2. Schematic illustration defining (a) Pb-edged and (b) Ti-edged fictitious unit cells used for the evaluation of local polarization in PbO-terminated and TiO<sub>2</sub>-terminated nanowires, respectively.

TABLE I. Local polarization evaluated via Eq. (1),  $P$  (in  $\mu\text{C}/\text{cm}^2$ ), of the edge, surface, and inside cells in the PbO-terminated and  $\text{TiO}_2$ -terminated nanowires with a  $4 \times 4$ -cell cross section. The results for  $[100]$ -polarized film with (001) surfaces (Ref. 22) and the bulk are shown for comparison. For the film, polarization is taken from the magnitude in the unit cell on the surface as the surface cell in the nanowire.

	Nanowire			Film	Bulk
	Edge cell	Surface cell	Inside cell		
PbO termination	103.2	96.5	81.0	93.8	85.8
$\text{TiO}_2$ termination	0.55	0.70	1.61	47.0	85.8

$$\mathbf{P} = \frac{e}{\Omega_c} \sum_j w_j \mathbf{Z}_j^* \mathbf{u}_j, \quad (1)$$

where  $\Omega_c$ ,  $e$ , and  $\mathbf{u}_j$  denote the volume of the unit cell, the electron charge, and the atomic displacement vector from the ideal lattice site of atom  $j$ , respectively. Index  $j$  runs over all atoms in the unit cell  $i$ .  $\mathbf{Z}_j^*$  is the Born effective charge tensor of the cubic bulk  $\text{PbTiO}_3$ . In this study, we used the theoretical values of the Born effective charge tensors calculated by Zhong *et al.*<sup>13</sup> Weights are set to  $w_{\text{Pb}}=1/8$ ,  $w_{\text{Ti}}=1$ , and  $w_{\text{O}}=1/2$  for the Pb-edged cell, and  $w_{\text{Pb}}=1$ ,  $w_{\text{Ti}}=1/8$ , and  $w_{\text{O}}=1/2$  for the Ti-edged cell. These correspond to the number of unit cells that share the atom. As this evaluation has already been validated in Refs. 30 and 31, spontaneous polarization of the bulk is evaluated to be  $85.8 \mu\text{C}/\text{cm}^2$  from Eq. (1) while the precise magnitude on the basis of the Berry phase theory<sup>32</sup> is  $78.6 \mu\text{C}/\text{cm}^2$ . Since the deviation is small (less than 10%), the simplified evaluation of local polarization is effective to qualitatively discuss the site-by-site ferroelectric distortions in nanowires.

Table I shows local polarization of the edge, surface, and inside cells in the PbO-terminated and  $\text{TiO}_2$ -terminated nanowires with the  $4 \times 4$ -cell cross section. The results of the  $[100]$ -polarized nine-layered  $\text{PbTiO}_3$  film with the (001) surfaces<sup>22</sup> and the bulk are shown for comparison. For the film, polarization is taken from the magnitude in the unit cell on the surface as the surface cell in the nanowire. In the PbO-terminated nanowire, the edge cell exhibits the highest local polarization. The local polarization of the surface cell,

which is second highest, is nearly equal to that of the film. Polarization in the inside cell is also comparable to that of the bulk. On the other hand, little polarization is found in the  $\text{TiO}_2$ -terminated nanowire. More specifically, the inner cell in the nanowire exhibits higher polarization, which is the opposite of the trend found in the PbO-terminated nanowire. Thus, ferroelectricity in the vicinity of the edge is enhanced in the PbO-terminated nanowire while it is considerably suppressed in the  $\text{TiO}_2$ -terminated nanowire. Note that the  $\text{TiO}_2$ -terminated nanowire shrinks in the  $z$  (axial) direction at equilibrium, resulting in considerable suppression of tetragonality,  $c/\bar{a}=0.973$  ( $c/a=1.043$  for bulk), where  $\bar{a}$  denotes the averaged lateral lattice parameter of the wire. It was reported that ferroelectricity in  $\text{PbTiO}_3$  is suppressed as uniaxial compression is applied along the  $c$  axis, meaning the decrease in tetragonality.<sup>33</sup> Hence, the tiny magnitude of polarization of the  $\text{TiO}_2$  termination even in the inside cell is due to not only the effect of  $\text{TiO}_2$ -terminated surface but also the highly reduced tetragonality.

It was both theoretically<sup>34</sup> and experimentally<sup>35</sup> revealed that the prominent ferroelectricity and large lattice tetragonality in  $\text{PbTiO}_3$  stem from the formation of the strong covalent Pb-O bond through the hybridization of the Pb  $6s$  and O  $2p$  orbitals, unlike  $\text{BaTiO}_3$  where the Ba-O interaction is almost ionic. In addition, the Pb-O bond often plays a significant role in determining characteristic structures, such as a complex  $c(2 \times 2)$  surface reconstruction<sup>22,23</sup> and an atomically sharp  $90^\circ$  domain-wall structure.<sup>30,31</sup> Thus, the Pb-O bond characterizes ferroelectric instability in  $\text{PbTiO}_3$ . Table II lists the bond length  $d$  and minimum charge density  $\rho_{\text{min}}$  of the edge, surface, and inside Pb-O bonds in both the PbO-

TABLE II. Bond length  $d$  (in angstroms), and minimum charge density  $\rho_{\text{min}}$  (in  $\text{\AA}^{-3}$ ), of the Pb-O covalent bond in the edge, surface, and inside cells. The corresponding Pb-O bonds in the bulk and on the (001) surface of the nine-layered film (Ref. 22) are shown for comparison.

	Nanowire			Film	Bulk
	Edge bond	Surface bond	Inside bond		
PbO termination					
$d$	2.243	2.299	2.464	2.386	2.506
$\rho_{\text{min}}$	0.534	0.473	0.332	0.392	0.312
$\text{TiO}_2$ termination					
$d$	2.675	2.722	2.697	2.631	2.506
$\rho_{\text{min}}$	0.230	0.203	0.216	0.240	0.312

terminated and  $\text{TiO}_2$ -terminated nanowires (see Fig. 1). The minimum charge density is calculated on a line between the bonded Pb and O atoms. For comparison, we also show those of the bonds in the bulk and in the film as mentioned above, whose sites correspond to the surface and inside bonds in the nanowire. In the PbO-terminated nanowire, the bond-length order is  $d^{(\text{edge})} < d^{(\text{surface})} (< d^{(\text{Film})}) < d^{(\text{inside})} (\approx d^{(\text{Bulk})})$ , and the minimum charge-density order is  $\rho_{\text{min}}^{(\text{edge})} > \rho_{\text{min}}^{(\text{surface})} > (\rho_{\text{min}}^{(\text{Film})}) > \rho_{\text{min}}^{(\text{inside})} (\approx \rho_{\text{min}}^{(\text{Bulk})})$ . These findings indicate that a highly strengthened covalent bond is formed at the edge. On the other hand,  $d$  and  $\rho_{\text{min}}$  are longer and lower than those of the bulk in the  $\text{TiO}_2$ -terminated nanowire, suggesting that the Pb-O bond is weakened. Therefore, the large (small) ferroelectric distortion in the edge cell arises from the strengthened (weakened) covalent Pb-O bond in the PbO-( $\text{TiO}_2$ -) terminated nanowire.

Figure 3 depicts the difference in site-by-site minimum charge density between the corresponding site of the bulk and those in the PbO-terminated and  $\text{TiO}_2$ -terminated nanowires. In the PbO-terminated nanowire, the charge density at the edge and surface Pb-O bonds increases while that of the Ti-O bond decreases. This indicates that the electrons transfer from the Ti-O site to the Pb-O site. Because the coordination number of the Pb atom at the edge is smaller than that of the bulk, the number of electrons contributing to the bond increases in the PbO-terminated nanowire. In fact, the Pb atoms associated with the edge, surface, and inside bonds form two, three, and four Pb-O bonds, respectively, which correspond well to the minimum charge density although the relationship is not simply linear (see Table II). Thus, the electron concentration on the edge bond due to the reduced coordination number results in locally enhanced ferroelectricity. On the other hand, charge density increases at the Ti-O bond, especially at the edge in the  $\text{TiO}_2$ -terminated nanowire, while it decreases at the Pb-O bond. The enhancement of the Ti-O bond can be explained in the same manner as that of the Pb-O bond in the PbO-terminated nanowire. As a result of the charge redistribution from the Pb-O site to Ti-O site in the nanowire, the covalent Pb-O bond is relatively weakened, leading to strong suppression of ferroelectricity. Thus, ferroelectricity in the  $\text{PbTiO}_3$  nanowire depends significantly on the terminations. Such termination dependence is different in the  $\text{BaTiO}_3$  nanowires, where ferroelectricity is suppressed in the BaO termination while it is enhanced in the  $\text{TiO}_2$  termination<sup>17</sup> because the Ba-O interaction is not covalent but almost ionic.<sup>34,35</sup>

### B. Effect of size on ferroelectricity

Table III lists the averaged lateral and the axial lattice parameters,  $\bar{a}$  and  $c$ , and the averaged polarization  $\bar{P}$  in both the PbO-terminated and  $\text{TiO}_2$ -terminated nanowires as a function of cross-sectional size. As the size of the PbO-terminated nanowire decreases, both the lateral and axial lattice parameters shrink. However, the tetragonality of lattice,  $c/\bar{a}$ , which plays an important role in stabilizing ferroelectric distortion, increases in the smaller nanowire. Surprisingly, even the smallest PbO-terminated nanowire with a  $1 \times 1$  unit-cell size exhibits spontaneous polarization, which has

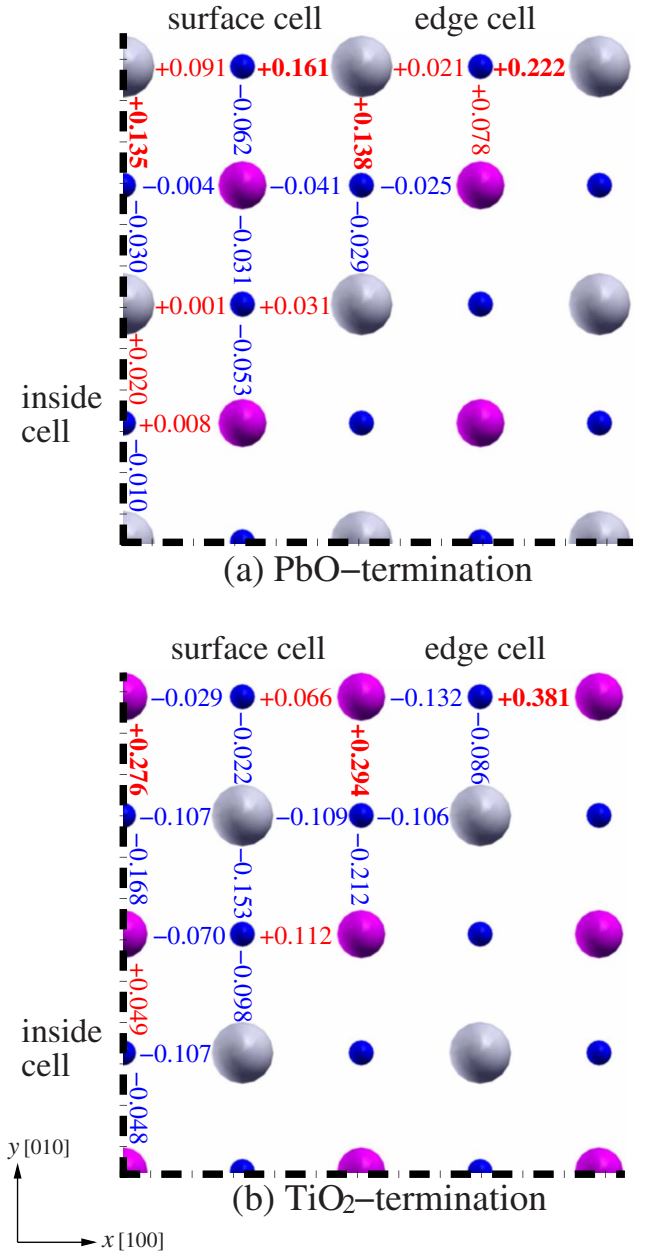


FIG. 3. (Color online) Difference in site-by-site minimum charge density from the corresponding site in the bulk in (a) PbO-terminated and (b)  $\text{TiO}_2$ -terminated nanowires with a  $4 \times 4$ -cell cross section (in  $\text{\AA}^{-3}$ ). The numbers in red (dark gray) and blue (black) indicate the increase and decrease, respectively. Only the top right quarter of the cross section is shown by symmetry.

the highest magnitude among the nanowires and bulk. This is because the ratio of the edge structure that enhances ferroelectricity with respect to the entire wire volume becomes more dominant with decreasing nanowire size. The magnitude of polarization approaches that of the bulk as the size increases. On the other hand, the lattice parameters of the smaller  $\text{TiO}_2$ -terminated nanowire also shrink but the tetragonality decreases because the axial lattice parameter is highly suppressed. Moreover, nanowires smaller than  $4 \times 4$  cells in cross section, which corresponds to a diameter of about  $17 \text{ \AA}$ , do not exhibit spontaneous polarization, indicat-

TABLE III. Averaged lateral and axial lattice parameters,  $\bar{a}$  and  $c$  (in angstroms), and averaged polarization  $\bar{P}$  (in  $\mu\text{C}/\text{cm}^2$ ), in both the PbO-terminated and TiO<sub>2</sub>-terminated nanowires as a function of cross-sectional size.

Nanowire size	1 × 1	2 × 2	3 × 3	4 × 4	Bulk
PbO termination					
$\bar{a}$	3.60	3.64	3.70	3.73	3.87
$c$	3.92	3.97	3.99	4.01	4.03
$c/\bar{a}$	1.088	1.090	1.081	1.074	1.043
$\bar{P}$	103.7	99.9	95.7	94.3	85.8
TiO <sub>2</sub> termination					
$\bar{a}$	3.77	3.81	3.84	3.85	3.87
$c$	3.39	3.57	3.67	3.74	4.03
$c/\bar{a}$	0.900	0.935	0.956	0.973	1.043
$\bar{P}$	0.00	0.00	0.00	0.89	85.8

ing that there is critical size for ferroelectricity. Such disappearance of ferroelectricity is also found in the stoichiometric BaTiO<sub>3</sub> nanowire surrounded by two BaO-terminated and two TiO<sub>2</sub>-terminated surfaces, and its critical size was calculated by Geneste *et al.*<sup>17</sup> to be 3 × 3 cells in cross section, which corresponds to a diameter of about 12 Å. They also demonstrated that the fully BaO-terminated (TiO<sub>2</sub>-terminated) BaTiO<sub>3</sub> nanowire requires the slightly larger (smaller) critical diameter. These indicate that critical size for ferroelectricity in perovskite nanowires is much sensitive to surface terminations, and the PbTiO<sub>3</sub> nanowire possesses relatively stronger dependence on surface terminations than the BaTiO<sub>3</sub> nanowire.

### C. Influence of axial tensile strain

Figure 4 plots the averaged polarization  $\bar{P}$  in the PbO-terminated and TiO<sub>2</sub>-terminated nanowires as a function of the tensile strain  $\epsilon_{zz}$ . Averaged polarization increases almost linearly with respect to tensile strain for all the PbO-terminated nanowires. This suggests that the axial tensile strain enhances the ferroelectricity. For the TiO<sub>2</sub>-terminated nanowires which are initially paraelectric (PE), ferroelectricity appears under axial tension. The critical tensile strain to recover ferroelectricity is listed in Table IV. Smaller nanowires require larger critical strain because the TiO<sub>2</sub>-terminated edge structure, which suppresses ferroelectricity, strongly affects thinner nanowires. After the critical strain, averaged polarization increases smoothly with tensile strain.

Figure 5 shows the change in atomistic and electronic configurations on the PbO (010) planes in the PbO-terminated and TiO<sub>2</sub>-terminated nanowires with a cross section of 3 × 3 unit cells under axial tension. At equilibrium in the PbO-terminated nanowire, O atoms are displaced in the  $-z$  direction from their ideal lattice sites and the covalent Pb-O bonds emphasized by white lines are formed, indicating ferroelectric distortion. During axial tension, all the Pb-O covalent bonds are sustained and the charge density at these

sites increases. On the other hand, the upper and lower Pb-O bonds are equivalent to each other and there is no ferroelectric distortion in the unstrained TiO<sub>2</sub>-terminated nanowire. After the critical strain of  $\epsilon_c=0.04$ , the upper bond is strengthened while the lower one is weakened for all the PbO planes accompanying the upward displacement of the

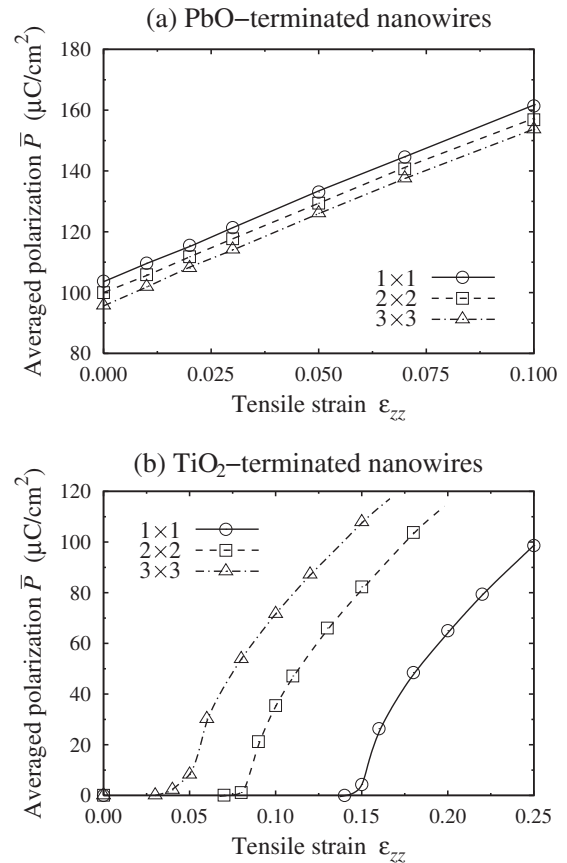


FIG. 4. Averaged polarization  $\bar{P}$  in (a) PbO-terminated and (b) TiO<sub>2</sub>-terminated nanowires with a cross section of the 1 × 1, 2 × 2, and 3 × 3 cells as a function of tensile strain  $\epsilon_{zz}$ .

TABLE IV. Critical tensile strain to recover ferroelectricity  $\epsilon_c$  as a function of the  $\text{TiO}_2$ -terminated nanowire size.

Nanowire size	$1 \times 1$	$2 \times 2$	$3 \times 3$
$\epsilon_c$	0.15	0.08	0.04

Pb atom. As a result, the nanowire undergoes a paraelectric-to-ferroelectric phase transition.

For more detailed discussion, we define the ‘‘edge,’’ ‘‘surface,’’ and ‘‘inside’’ bonds in the  $3 \times 3$  nanowire (see Fig. 5) in the same manner as in the  $4 \times 4$  nanowire. Figure 6 plots the minimum charge density,  $\rho_{\min}$ , at the edge, surface, and inside bonds in the PbO-terminated and  $\text{TiO}_2$ -terminated nanowires with a cross section of  $3 \times 3$  cells as a function of axial tensile strain  $\epsilon_{zz}$ . The minimum charge density at each

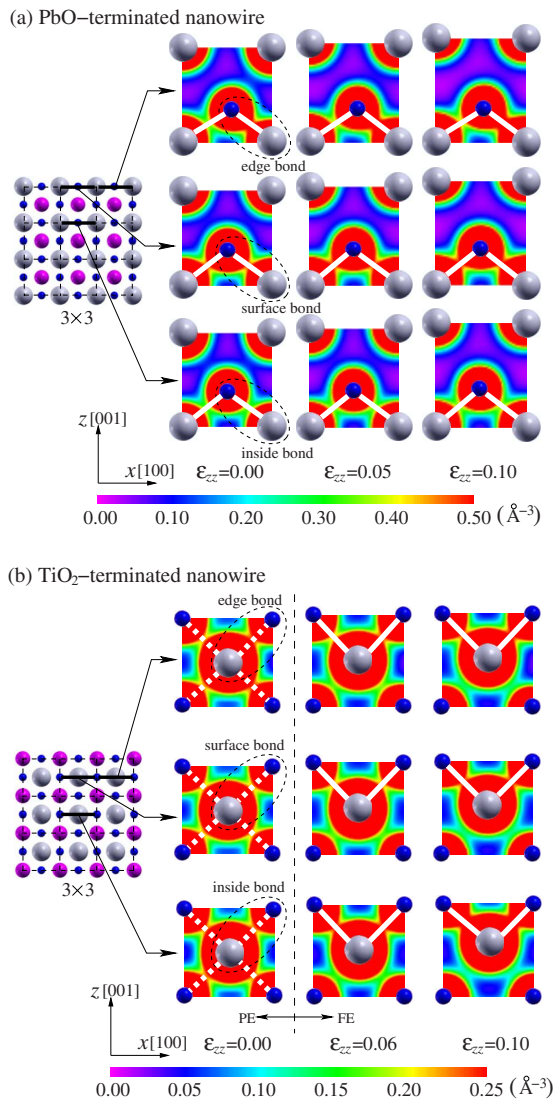


FIG. 5. (Color online) Change in atomic structures and charge-density distributions on the PbO (010) planes in (a) PbO-terminated and (b)  $\text{TiO}_2$ -terminated nanowires with a cross section of  $3 \times 3$  unit cells under axial tensile strain  $\epsilon_{zz}$ . The gray (dark gray) and blue (black) spheres indicate Pb and O atoms, respectively. The covalent Pb-O bonds are shown by white lines.

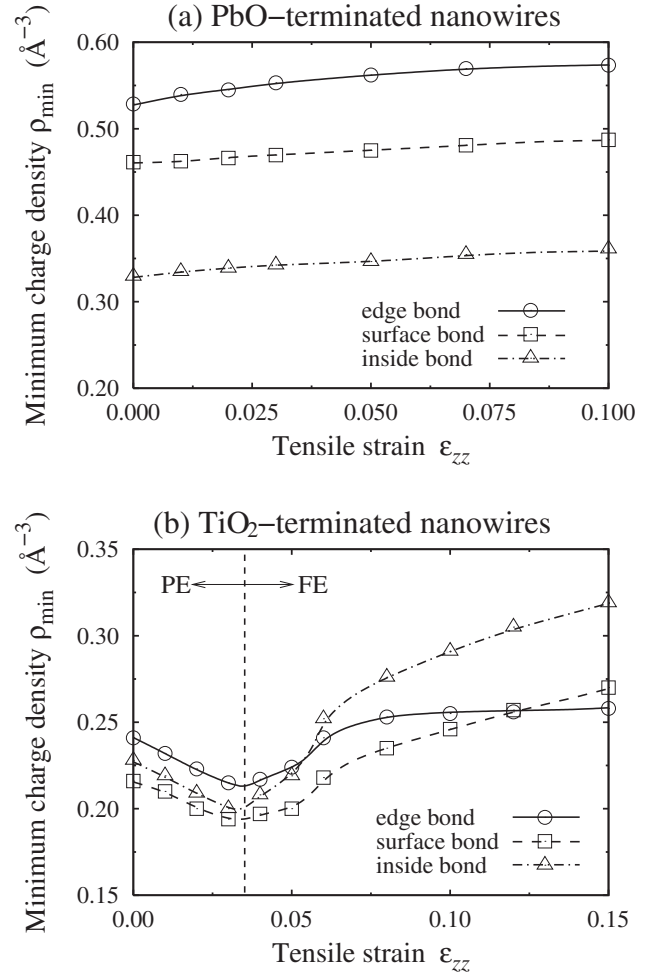


FIG. 6. Minimum charge density  $\rho_{\min}$  at the edge, surface, and inside bonds (see Fig. 5) in (a) PbO-terminated and (b)  $\text{TiO}_2$ -terminated nanowires with a  $3 \times 3$ -cell cross section as a function of axial tensile strain  $\epsilon_{zz}$ . The dashed line indicates the critical strain of the PE-FE phase transition.

bond increases monotonically with respect to the tensile strain in the PbO-terminated nanowire. This corresponds well to the linear increase in the averaged polarization. Under high axial tension, the edge bond keeps the highest charge density of the three. In the  $\text{TiO}_2$ -terminated nanowire, the minimum charge density decreases before the critical strain. This indicates that the equivalent bonds at the upper and lower sites of the PbO plane are uniformly stretched because the structure is paraelectric (symmetric in the  $z$  direction). At the critical strain, the trend for all the bonds concurrently changes from decreasing to increasing. This indicates that ferroelectricity appears in all the sites of the nanowire at the same strain, whereas the ferroelectric distortions in the  $\text{BaTiO}_3$  nanowire do not emerge for the same tension at the different site.<sup>17</sup> After that, all the upper bonds are partially strengthened. Note that the charge density increase in the edge bond is somewhat moderate, which leads to the suppression of ferroelectricity at the edge relative to the other sites.

#### IV. CONCLUSION

*Ab initio* density-functional theory calculations within the local-density approximation have been carried out in order to investigate the atomistic and electronic structures of  $\text{PbTiO}_3$  nanowires with atomically sharp edges composed of (100) and (010) surfaces, and the fundamental effects of axial tensile strain on ferroelectricity. Ferroelectric distortions at the edge of the  $\text{PbO}$ -terminated nanowire are enhanced while they are entirely suppressed in the  $\text{TiO}_2$ -terminated nanowire. On the other hand, an opposite trend of termination dependence is observed for the  $\text{BaTiO}_3$  nanowire.<sup>17</sup>

We have shown that ferroelectricity is enhanced as a result of the formation of strong  $\text{Pb-O}$  covalent bonds at the edge of the  $\text{PbO}$ -terminated nanowire. This arises from the increase in electrons contributing to the bond due to the relative decrease in the coordination number of the  $\text{Pb}$  atom. In the  $\text{TiO}_2$ -terminated nanowire, the  $\text{Pb-O}$  bonds are weakened by the charge transfer from the  $\text{Pb-O}$  site to the  $\text{Ti-O}$  site.

Surprisingly, the smallest  $\text{PbO}$ -terminated nanowire with a cross section of only one-unit cell exhibits spontaneous polarization, which has a higher magnitude than the bulk. By contrast, the  $\text{TiO}_2$ -terminated nanowires with a cross section smaller than  $4 \times 4$  cells (about 17 Å in a diameter) cannot sustain ferroelectricity, indicating the existence of critical size. For the  $\text{BaTiO}_3$  nanowires, the critical size for ferroelectricity also exists and it depends on surface termination. However, the trend is different from that of the  $\text{PbTiO}_3$  nanowire; the  $\text{BaO}$ -terminated nanowire requires the larger criti-

cal diameter while the diameter is smaller in the  $\text{TiO}_2$  termination.<sup>17</sup>

Spontaneous polarization in the  $\text{PbO}$ -terminated nanowires increases almost proportionally to the applied tensile strain accompanying the homogeneous enhancement of the  $\text{Pb-O}$  bond. In the  $\text{TiO}_2$ -terminated nanowires, which are initially paraelectric, the ferroelectricity emerges under axial tension. A larger critical strain is required for smaller nanowires, where the suppressing effect of the edge on ferroelectricity becomes predominant. After the critical strain, the  $\text{Pb-O}$  bond at the edge exhibits moderate enhancement compared with the other bonds. This leads to the relative suppression of ferroelectricity at the edge.

In this paper, we simulated the nanowires with the periodicity of one-unit cell in the axial direction. Considering the  $c(2 \times 2)$  reconstruction of the (001) surface,<sup>22,23</sup> there are possibilities of existence of the reconstruction even in the  $\text{PbTiO}_3$  nanowires, and this remains as challenging future work. We believe that our results are helpful as a criterion in discussing the basic influence of the  $c(2 \times 2)$  reconstruction if it exists in the nanowires.

#### ACKNOWLEDGMENT

This work was supported in part by a Grant-in-Aid for Scientific Research (S) (Grant No. 16106002), of the Japan Society of the Promotion of Science.

\*shimada@cyber.kues.kyoto-u.ac.jp

<sup>1</sup>J. F. Scott, *Ferroelectric Memories* (Springer, Berlin, 2000).

<sup>2</sup>R. Ramesh, *Thin Film Ferroelectric Materials and Devices* (Kluwer Academic, Boston, 1997).

<sup>3</sup>H. Gu, Y. Hu, J. You, Z. Hu, Y. Yuan, and T. Zhang, *J. Appl. Phys.* **101**, 024319 (2007).

<sup>4</sup>W. S. Yun, J. J. Urban, Q. Gu, and H. Park, *Nano Lett.* **2**, 447 (2002).

<sup>5</sup>J. J. Urban, W. S. Yun, Q. Gu, and H. Park, *J. Am. Chem. Soc.* **124**, 1186 (2002).

<sup>6</sup>Y. Yamashita, K. Mukai, J. Yoshinobu, M. Lippmaa, T. Kinoshita, and M. Kawasaki, *Surf. Sci.* **514**, 54 (2002).

<sup>7</sup>G. B. Cho, M. Yamamoto, and Y. Endo, *Thin Solid Films* **464**, 80 (2004).

<sup>8</sup>K. Takahashi, M. Suzuki, M. Yoshimoto, and H. Funakubo, *Jpn. J. Appl. Phys., Part 2* **45**, L138 (2006).

<sup>9</sup>E. A. Kotomin, E. Heifets, S. Dorfman, D. Fuks, A. Gordon, and J. Maier, *Surf. Sci.* **566-568**, 231 (2004).

<sup>10</sup>M. W. Chu, I. Szafraniak, R. Scholz, C. Harnagea, D. Hesse, M. Alexe, and U. Gosele, *Nature Mater.* **3**, 87 (2004).

<sup>11</sup>J. H. Jeon and S. K. Choi, *Appl. Phys. Lett.* **91**, 091916 (2007).

<sup>12</sup>R. Resta, M. Posternak, and A. Baldereschi, *Phys. Rev. Lett.* **70**, 1010 (1993).

<sup>13</sup>W. Zhong, R. D. King-Smith, and D. Vanderbilt, *Phys. Rev. Lett.* **72**, 3618 (1994).

<sup>14</sup>M. E. Lines and A. M. Glass, *Principles and Applications of Ferroelectrics and Related Materials* (Oxford University Press, Oxford, 2001).

<sup>15</sup>O. Diéguez, S. Tinte, A. Antons, C. Bungaro, J. B. Neaton, K. M.

Rabe, and D. Vanderbilt, *Phys. Rev. B* **69**, 212101 (2004).

<sup>16</sup>K. M. Rabe, *Curr. Opin. Solid State Mater. Sci.* **9**, 122 (2005).

<sup>17</sup>G. Geneste, E. Bousquet, J. Junquera, and P. Ghosez, *Appl. Phys. Lett.* **88**, 112906 (2006).

<sup>18</sup>P. Hohenberg and W. Kohn, *Phys. Rev.* **136**, B864 (1964).

<sup>19</sup>W. Kohn and L. Sham, *Phys. Rev.* **140**, A1133 (1965).

<sup>20</sup>P. Ghosez, E. Cockayne, U. V. Waghmare, and K. M. Rabe, *Phys. Rev. B* **60**, 836 (1999).

<sup>21</sup>B. Meyer, J. Padilla, and D. Vanderbilt, *Faraday Discuss.* **114**, 395 (1999).

<sup>22</sup>Y. Umeno, T. Shimada, T. Kitamura, and C. Elsässer, *Phys. Rev. B* **74**, 174111 (2006).

<sup>23</sup>C. Bungaro and K. M. Rabe, *Phys. Rev. B* **71**, 035420 (2005).

<sup>24</sup>R. I. Eglitis and D. Vanderbilt, *Phys. Rev. B* **76**, 155439 (2007).

<sup>25</sup>G. Kresse and J. Hafner, *Phys. Rev. B* **47**, 558 (1993).

<sup>26</sup>G. Kresse and J. Furthmüller, *Phys. Rev. B* **54**, 11169 (1996).

<sup>27</sup>P. E. Blöchl, *Phys. Rev. B* **50**, 17953 (1994).

<sup>28</sup>D. M. Ceperley and B. J. Alder, *Phys. Rev. Lett.* **45**, 566 (1980).

<sup>29</sup>H. J. Monkhorst and J. D. Pack, *Phys. Rev. B* **13**, 5188 (1976).

<sup>30</sup>B. Meyer and D. Vanderbilt, *Phys. Rev. B* **65**, 104111 (2002).

<sup>31</sup>T. Shimada, Y. Umeno, and T. Kitamura, *Phys. Rev. B* **77**, 094105 (2008a).

<sup>32</sup>R. Resta, *J. Phys.: Condens. Matter* **12**, R107 (2000).

<sup>33</sup>T. Shimada, K. Wakahara, Y. Umeno, and T. Kitamura, *J. Phys.: Condens. Matter* **20**, 325225 (2008b).

<sup>34</sup>R. E. Cohen, *Nature (London)* **358**, 136 (1992).

<sup>35</sup>Y. Kuroiwa, S. Aoyagi, A. Sawada, J. Harada, E. Nishibori, M. Takata, and M. Sakata, *Phys. Rev. Lett.* **87**, 217601 (2001).